ELSEVIER

Modeling coupled interactions of carbon, water, and ozone exchange between terrestrial ecosystems and the atmosphere. I: Model description

Ned Nikolov[a,*], Karl F. Zeller[b]

[a]N & T Services, 6736 Flagler Road, Fort Collins, CO 80525, USA
[b]US FS Rocky Mountain Station, 240 West Prospect Rd., Fort Collins, CO 80526, USA

"Capsule": *A new biophysical model (FORFLUX) is presented to link ozone deposition with carbon and water cycles in terrestrial ecosystems.*

Abstract

A new biophysical model (FORFLUX) is presented to study the simultaneous exchange of ozone, carbon dioxide, and water vapor between terrestrial ecosystems and the atmosphere. The model mechanistically couples all major processes controlling ecosystem flows trace gases and water implementing recent concepts in plant eco-physiology, micrometeorology, and soil hydrology. FORFLUX consists of four interconnected modules—a leaf photosynthesis model, a canopy flux model, a soil heat-, water- and CO_2- transport model, and a snow pack model. Photosynthesis, water–vapor flux and ozone uptake at the leaf level are computed by the LEAFC3 sub-model. The canopy module scales leaf responses to a stand level by numerical integration of the LEAFC3 model over canopy leaf area index (LAI). The integration takes into account (1) radiative transfer inside the canopy, (2) variation of foliage photosynthetic capacity with canopy depth, (3) wind speed attenuation throughout the canopy, and (4) rainfall interception by foliage elements. The soil module uses principles of the diffusion theory to predict temperature and moisture dynamics within the soil column, evaporation, and CO_2 efflux from soil. The effect of soil heterogeneity on field-scale fluxes is simulated employing the Bresler–Dagan stochastic concept. The accumulation and melt of snow on the ground is predicted using an explicit energy balance approach. Ozone deposition is modeled as a sum of three fluxes– ozone uptake via plant stomata, deposition to non-transpiring plant surfaces, and ozone flux into the ground. All biophysical interactions are computed hourly while model projections are made at either hourly or daily time step. FORFLUX represents a comprehensive approach to studying ozone deposition and its link to carbon and water cycles in terrestrial ecosystems.
© 2003 Elsevier Science Ltd. All rights reserved.

Keywords: Biophysical model; Trace gas; Flux; Photosynthesis; Pollutant; Ozone; Deposition

1. Introduction

The seasonal exchange of trace gases (e.g. CO_2, ozone, etc.) and water vapor between terrestrial ecosystems and the atmosphere is a key aspect of the functioning of the Earth's Biosphere. At the regional scale, this exchange controls ecosystem productivity and influences meso-scale atmospheric circulation and weather patterns (Pielke and Avissar, 1990; Henderson-Sellers and Pitman, 1992). The temporal dynamics of the ecosystem-atmosphere mass and energy exchange is governed by a diverse array of physiological and biophysical processes. Understanding these biogeophysical interactions is critical to our ability to predict long-term effects of directional changes in climatic on forest ecosystems as well as to assess functional feedbacks between landscape distribution of forests and mesoscale climate.

Over the past 20 years, numerous models were proposed to study biophysical transport of trace gases, water and energy between land surface and the atmosphere. Some models were specifically developed as simulators of the lower-boundary conditions in climate

---

* Corresponding author. Tel.: +1-970-980-3303.
E-mail addresses: ntconsulting@attbi.com (N. Nikolov), kzeller@fs.fed.us (K. F. Zeller).

models (e.g. Sellers et al., 1986; Dickinson et al., 1993) while others were designed to primarily aid ecosystem research, e.g. FOREST-BGC (Running and Coughlan, 1988; Running and Gower, 1991), BIOMASS (McMurtie et al., 1990, 1992), TXT (Bonnan, 1991a,b), PnET (Aber and Federrer, 1992), and GEMTM (Chen and Coughenour, 1994). Although most biophysical models adopt a similar overall structure, there are significant differences in the details of the schemes employed to predict various fluxes. These disparities mainly pertain to four aspects of model algorithms: (1) the use of single-, dual-, or multiple-source formulations to estimate mass and energy fluxes from the canopy and soil; (2) the presence or lack of a mechanistic coupling between trace gas uptake, plant transpiration and heat exchange; (3) the implementation of process-based versus empirical relationships to describe combined responses of leaf stomatal conductance and net photosynthesis to variations in ambient meteorological conditions; and (4) the utilization of physical diffusion principles as opposed to "soil-bucket" approximations to simulate soil moisture and temperature dynamics.

We present here a new biogeo-physical model named FORFLUX to simulate the diurnal and seasonal dynamics of carbon, ozone, and water fluxes in terrestrial ecosystems. The model incorporates a multi-layer canopy and soil schemes, and uses an improved mathematical description of leaf, canopy and soil processes. It also incorporates a new root–shoot communication algorithm based on recent findings of plant physiology and soil hydrology. The model represents a comprehensive approach to studying ozone deposition and its link to carbon and water cycles. For the first time, vegetation ozone uptake is coupled to carbon assimilation and evapo-transpiration through the function of leaf stomata. This paper describes the ecosystem-atmosphere interactions as formulated in FORFLUX, and model input parameters and output variables. A companion publication focuses on model verification and presents a FORFLUX application investigating the functional sensitivity of a subalpine forest ecosystem in southern Wyoming (USA) to variations in key climatic and vegetation parameters.

2. The FORFLUX Model

FORFLUX is a one-dimensional point model, which simulates seasonal dynamics of carbon dioxide (CO_2), ozone (O_3), and water–vapor exchange between a terrestrial ecosystem and the atmosphere (Nikolov, 1997; Zeller and Nikolov, 2000). FORFLUX consists of four interconnected modules: a leaf photosynthesis model, a canopy flux model, a soil heat, water and CO_2 transport model and a snow-pack model. All biophysical interactions are computed hourly while model projections are

provided at hourly or daily time step. Fig. 1 portrays the main modules, their interaction and order of execution.

FORFLUX requires input data on weather, soils, species eco-physiology, and vegetation stand structure. Meteorological forcing includes hourly values of ambient temperature, relative humidity, incoming total short-wave radiation, precipitation and above-canopy wind speed. Soil is described by texture, depth, and volumetric rock content. Canopy leaf area index (LAI) and foliage clumping factor (CF) define stand structure. Species physiology is characterized in the model by 20 parameters (see discussion below). Model output includes temporal courses of net ecosystem carbon, water, and ozone fluxes and their components, such as vegetation net primary production (NPP), plant ozone uptake, canopy photosynthesis and stomatal conductance, woody respiration, soil CO_2 efflux, canopy transpiration and rainfall interception, soil evaporation,
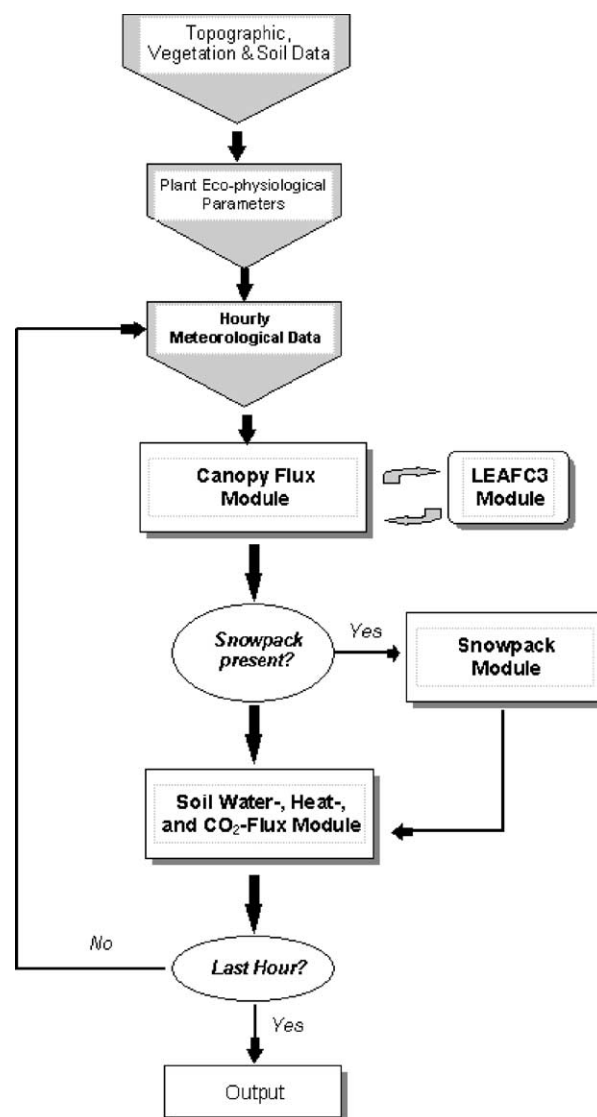

Fig. 1. Flow diagram of the FORFLUX model.

snow melt and sublimation, surface runoff and subsoil drainage.

In its current version, the FORFLUX model does not include a mechanistic representation of nutrient cycling. The later has been omitted on the assumption that short-term (i.e. diurnal to seasonal) variations of eco-system fluxes are primarily controlled by meteorological and plant-physiological factors. Nutrient availability typically affects ecosystem dynamics over temporal scales of decades or longer. The following sections describe the FORFLUX modules in greater detail.

2.1. Leaf level processes

Leaf surface is the arena where trace gas exchange interacts most closely with plant water loss. This inter-action involves physical processes of leaf energy balance and leaf physiological responses such as stomatal movement and intracellular biochemical reactions. Nikolov et al. (1995) combined functional relationships from leaf physiology, biophysics, and fluid mechanics to developed a generic photosynthesis model (LEAFC3), which predicts instantaneous steady-state fluxes of CO_2, water vapor, and heat from broad leaves and needle-leaved coniferous shoots of C_3 plants. Fig. 2 depicts input and output variables and process interactions in the LEAFC3 model. FORFLUX uses LEAFC3 to pre-dict leaf-level fluxes.

LEAFC3 requires input data on absorbed short- and long-wave radiation by the leaf, ambient air tempera-ture, humidity, wind speed, atmospheric concentrations of CO_2 and O_2, and barometric pressure. These data are

provided by the Canopy Flux module. A set of ten input parameters is used to characterize leaf eco-physiological properties such as potential rate of carboxylation and electron transport (see Table 1). The model predicts four state variables which are supplied as input to the canopy portion of the FORFLUX model, i.e. net pho-tosynthesis rate (A_n µmol m^{-2} s^{-1}), stomatal con-ductance to water vapor and ozone (g_{sv} µmol m^{-2} s^{-1}), leaf temperature (T_1 °C), and leaf boundary-layer con-ductance (g_{bv} µmol m^{-2} s^{-1}). These variables are esti-mated as a solution to a system of four simultaneous equations of the following general form:

$$A_n = f(g_{sv}, g_{bv}, T_1)$$

$$g_{sv} = f(A_n, g_{bv}, T_1)$$

$$T_1 = f(g_{sv}, g_{bv})$$

$$g_{bv} = f(T_1)$$

Equations for A_n and T_1 are quartic while that for g_{sv} is quadratic (for more information about deriva-tion and solution of these equations, see Nikolov et al. 1995, pp. 212–214). Latent heat flux (i.e. transpira-tion) is estimated from predicted leaf temperature and leaf-surface conductances using a standard flux–resis-tance relationship.

The main advantage of the LEAFC3 model over other more empirical photosynthesis models (e.g. Jarvis, 1976) is that it explicitly accounts for feedbacks between
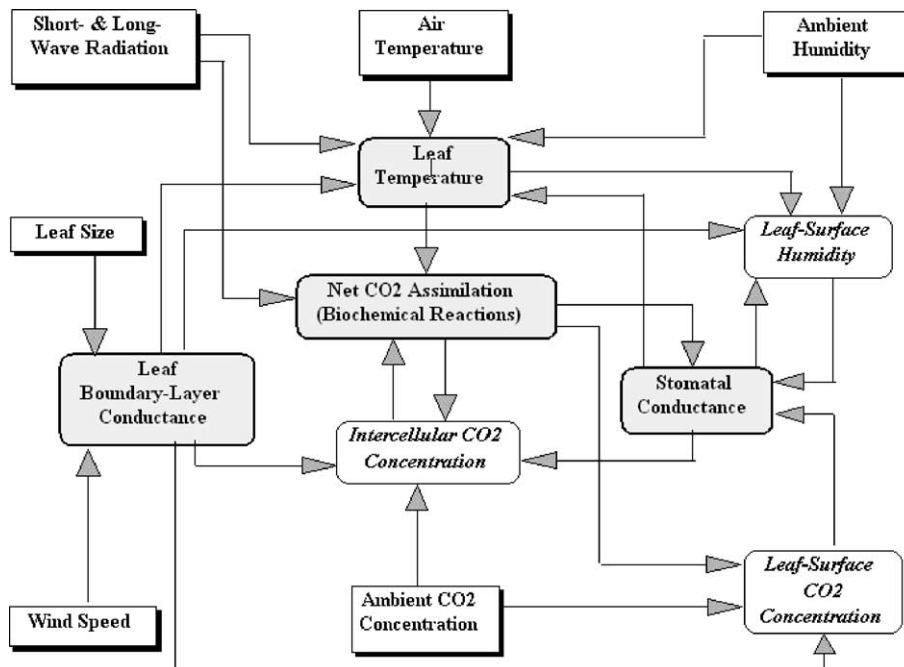

Fig. 2. Input and output variables and process interactions in the LEAFC3 model.

leaf energy balance, stomatal conductance, and CO_2 assimilation processes.

The FORFLUX model implements an improved version of LEAFC3, which differs from the one presented by Nikolov et al. (1995) in the following: (1) Equation describing the impact of leaf water potential on stomatal conductance (p. 209 in Nikolov et al.) was replaced by a function that simulates the combined influence of root hydraulic and chemical signaling on leaf stomatal aperture. The new root–shoot communication algorithm (discussed below) is based on data and models by Tardieu et al. (1993) and Tardieu and Davis (1993a,b). (2) The temperature response functions for the potential rate of electron transport (J_{max}) and carboxylation velocity (V_{max}) were replaced with more realistic (less extreme) curves. (3) A temperature acclimation function has been incorporated for V_{m25} and J_{m25} (Table 1). These species parameters are now updated daily throughout the season as a function of average ambient temperature over the past 7 days. The variation of V_{m25} and J_{m25} is relative to a species-specific summer maximum value.

2.2. Canopy processes

The FORFLUX canopy module predicts the exchange of CO_2, ozone, and water vapor between the above-ground portion of a vegetation stand and the atmosphere. Canopy photosynthesis and evapo-transpiration are estimated by combining the LEAFC3 model with algorithms which simulate (1) short- and long-wave radiative transfer inside the canopy, (2) variation of foliage photosynthetic capacity with canopy depth, (3) wind speed attenuation throughout the canopy, and (4) rainfall interception by foliage elements. The canopy submodel also computes aboveground woody respiration and seasonal phenological changes in stand leaf area index (LAI).

2.2.1. Radiative transfer

The total short-wave solar radiation provided as input to the model is decomposed into incident direct and diffuse fluxes in the visible and near-infrared band. Radiation components are estimated as functions of solar elevation, ratio of extraterrestrial to surface radiation, cloudiness, and slope inclination and aspect of the site using equations and algorithms by Spitters et al. (1986), Perez (1990) and Nikolov and Zeller (1992). The radiative transfer algorithm inside the canopy implements a two-stream analytical solution to the multiple scattering equation. It is based on work by Ross (1981), Sellers (1985), and Camillo (1987). The algorithm accounts for spectral changes of the incident solar flux inside the canopy caused by the selective electromagnetic absorption of green leaves. The model uses leaf clumping and angular distribution of foliage elements to estimate penetration and absorption of direct and diffuse radiatiative fluxes in the visible (380–700 nm), near-infrared (700–1500 nm) and thermal (>1500 nm) band.

The transfer of short-wave radiation within a vegetation canopy is described by the ordinary differential equation developed by Ross (1981) and solved analytically by Sellers (1985) and Camillo (1987). The solution derived by Camillo (1987) is theoretically more robust since it explicitly accounts for non-isotropic radiation scatter by individual leaves. However, this solution is only valid for solar zenith angles smaller than 60°. FORFLUX computes short-wave radiative transfer by combining the analytical solutions provided by Camillo (1987) and Sellers (1985) into a single radiative transfer algorithm, which also accounts for the effect of foliage clumping. The canopy-clumping factor (Ω_{cl}) is a coefficient between 0.0 and 1.0 that quantifies the degree of aggregation of individual leaves into shoots, crown, and vegetation patches. In real stands, canopy clumping typically ranges between 0.5 and 0.95. The limited amount of data available on clumping suggests that Ω_{cl} declines exponentially with stand LAI (e.g. Sampson and Smith, 1993). This relationship has been incorporated into FORFLUX.

Upon entering plant canopy, the direct solar radiation splits into a downward beam, and upward and downward diffuse fluxes caused by the scatter of the direct

Table 1
Main species physiological input parameters of the FORFLUX model

Parameter	Symbol	Units
Maximum carboxylation velocity at 25 °C	V_{m25}	micromol m^{-2} s^{-1}
Light-saturated potential rate of electron transport	J_{m25}	micromol m^{-2} s^{-1}
Activation energy for electron transport	E_j	J/mol
Kinetic parameter for CO_2 at 25 °C	K_{c25}	mol/mol
Kinetic parameter for O_2 at 25 °C	K_{o25}	mol/mol
Photosynthetic light loss factor	f	dec. fraction
Composite stomatal sensitivity	m	dimensionless
Empirical constant for stomatal conductance	b_{sv}	mol m^{-2} s^{-1}
Mean needle width	d	m
Critical temperature for root conductance	T_{cr}	°C

beam. The attenuation of the beam part of the incident direct flux inside the canopy is predicted by the Beer–Lambert exponential formula:

$$Q^\downarrow(L) = \exp[-K\Omega_{cl}L] \tag{1}$$

where $Q^\downarrow(L)$ is the beam flux under leaf area index L normalized by the incident direct flux above the canopy, and K is the beam extinction coefficient of the canopy. By definition $K = G(u_o)/u_o$ where $G(u_o)$ is the ratio of projected to total leaf area in direction $u_o = \cos\theta_{sun}$. For canopies with spherical leaf angle distribution, $G(u_o) = 0.5$. For non-spherical canopies $G(u_o)$ varies with solar elevation. In FORFLUX, K is estimated using the ellipsoidal leaf-angle distribution model of Campbell (1986), i.e.

$$K = \frac{G(u_o)}{u_o} = \frac{[u_o^2(\chi^2 - 1) + 1]^{0.5}}{u_o[\chi + 1.744(\chi + 1.182)^{-0.733}]} \tag{2}$$

In this equation, χ is the ratio of vertical to horizontal projection of a representative volume of foliage. For canopies with spherical leaf angle distribution $\chi = 1$, for planophile canopies $\chi > 1$, and for erectophile canopies $\chi < 1$. Using results from a numerical integration of Campbell's ellipsoidal angle density function (Campbell, 1990), Wang and Jarvis (1988) derived an empirical equation relating χ to the canopy mean leaf inclination angle (Θ), i.e.

$$\chi = \begin{cases} 151.515\dfrac{1 - 0.0107\Theta}{\Theta} & \text{if } \Theta \geqslant 57.4° \\ 97.087\dfrac{1 - 0.0053\Theta}{\Theta} & \text{if } \Theta < 57.4° \end{cases} \tag{3}$$

For spherical canopies $\Theta = 57.4°$, for planophile canopies $0° < \Theta < 57.4°$, and for erectophile canopies $57.4° < \Theta < 90°$.

The normalized upward ($I_d^\uparrow$) and downward ($I_d^\downarrow$) hemispherical fluxes of diffuse radiation under LAI of L due to the scatter of the direct beam are derived from the particular solution to the ordinary differential equation by Ross (1981), i.e.

$$I_d^\downarrow(L) = h_4 Q^\downarrow(L) + h_5\exp(-h_o\,\Omega_{cl}L) + h_6\exp(h_o\Omega_{cl}L) \tag{4}$$

and

$$I_d^\uparrow(L) = h_1\,Q^\downarrow(L) + h_2\exp(-h_o\Omega_{cl}L) + h_3\exp(-h_o\Omega_{cl}L) \tag{5}$$

In these equations, coefficients h_i are functions of leaf optical properties (i.e. reflectance and transmittance), ground reflectivity (α_s), total stand LAI (L_{tot}), solar zenith angle (θ_{sun}), and foliage clumping. For brevity, we will not discuss the mathematical expressions for computing these coefficients here.

The normalized upward ($I_f^\uparrow$) and downward ($I_f^\downarrow$) hemispherical radiative fluxes under LAI of L due to the penetration and scatter of the incident diffuse radiation are derived from the homogeneous solution to the radiative transfer equation by Ross (1981), i.e.

$$I_f^\uparrow(L) = h_7\exp(-0.5h_o\Omega_{cl}L) + h_8\exp(0.5h_o\Omega_{cl}L) \tag{6}$$

and

$$I_f^\downarrow(L) = h_9\exp(-0.5h_o\Omega_{cl}L) + h_{10}\exp(0.5h_o\Omega_{cl}L) \tag{7}$$

where coefficients h_7 through h_{10} are functions of leaf optical characteristics, soil reflectance, total stand LAI, and foliage clumping.

The energy balance of plant canopies is significantly influenced by thermal radiative fluxes emitted from soil and the atmosphere as they interact with long-wave emissions from foliage and stems. The transport of thermal radiation inside the canopy is modeled using a two-stream approximation based on the following assumptions: (1) the sky is an isotropic source of long-wave emission; (2) the thermal scattering coefficients of soil, foliage and stems are effectively zero (i.e. long-wave radiation is not reflected or transmited by material objects); and (3) the thermal emission from plants can be approximated using ambient air temperature instead of actual tissue temperature. Following Ross (1981), the downward ($I_{lw}^\downarrow$) and upward ($I_{lw}^\uparrow$) long-wave radiative fluxes under LAI of L are computed as follows:

$$I_{lw}^\downarrow(L) = E_f + (E_a - E_f)a_D(L) \tag{8}$$

and

$$I_{lw}^\uparrow(L) = E_f + (E_s - E_f)a_D(L_{tot} - L) \tag{9}$$

where E_a is the down-welling thermal flux from the atmosphere, E_f is the long-wave emission from foliage, E_s is the emission from the ground (i.e. soil or snow-pack), and $a_D(X)$ is a penetration function defining the relative contribution of atmospheric and ground fluxes to the total thermal flux at a canopy depth L. The thermal fluxes E_i (W m^{-2}) in the above equations are estimated as

$$E_i = \varepsilon_i\sigma(T_i + 273.16)^4 \tag{10}$$

where ε_i is the emissivity of the corresponding object (i.e. atmosphere, foliage, soil, or snow), σ is the Stefen-Boltzmann constant (i.e. 5.67×10^{-8} W m^{-2} K^{-4}), and T_i is the surface temperature (°C) of the object (for foliage and stems, T_i equals ambient air temperature). The model assumes that $\epsilon = 0.975$ for foliage, $\epsilon = 0.95$ for soil, and $\epsilon = 0.99$ for snow. The emissivity of the atmosphere (ϵ_a) varies as a function of vapor pressure

(e_o, Pa), air temperature (T_a,°C), site altitude (Z, m), barometric pressure (P_a, Pa), and cloud cover (C_l, fraction). FORFLUX computes atmospheric emissivity (ϵ_a) combining equations by Brutsaert (1975), Marks and Dozier (1979) and Heitor et al. (1991), i.e.

$$\varepsilon_a = 0.642\left(\frac{1.38e_o}{T_a + 0.0068Z + 273.16}\right)^{\frac{1}{7}} \frac{P_a}{P_o}(1 + 0.23Cl)$$
(11)

where P_o is the sea-level (standard) barometric pressure (i.e. 101,325 Pa), and P_a is determined from the actual pressure at the site.

Atmospheric emissivity typically ranges from 0.65 (for clear sky and low humidity) to about 0.98 (for overcast sky and high humidity).

2.2.2. Variation of foliage photosynthetic capacity within the canopy

A decline of area-based foliage photosynthetic capacity with canopy depth has been observed in many vegetation stands (e.g. Hirose et al., 1988; Oren et al., 1986; Leuning, 1991; Ellsworth and Reich, 1993). It is currently believed that an enhanced concentration of CO_2-capturing resources near the top of plant canopies represents an evolutionary adaptation toward maximization of carbon gain (e.g. Field, 1983, Hirose and Werger, 1987; Wu, 1994). The vertical variation of carbon assimilation potential throughout the canopy appears to be far more pronounced in broad-leaved vegetation than it is in conifer stands (Schoettle, 1989; Brooks et al., 1997; Barbara Yoder, personal communication).

The FORFLUX model simulates changes of foliage photosynthetic capacity as a function of downward commutative LAI employing a formulation by Hirose and Werger (1987) and Hirose et al. (1988), i.e.

$$P_r(L) = \exp\left(-K_p \frac{L}{L_{tot}}\right)$$
(12)

where $P_r(L)$ is the fractional decline of Rubisco activity (V_{m25}) and the potential rate of electron transport (J_{m25}) of foliage under LAI of L relative to that at the canopy top, and K_p is an attenuation parameter depending on plant species and stand LAI. For closed canopies of broad-leaved species, often $0.6 \leqslant K_p \leqslant 0.8$. In the FORFLUX model, K_p is computed as a linear function of L_{tot}, i.e. $K_p = a_p + b_p\Omega_{cl}L_{tot}$, where a_p and b_p are species-specific parameters. The nominal values for these parameters are $a_p = 0.41$ and $b_p = 0.06$ for broad-leaved vegetation, and $a_p = 0.03$ and $b_p = 0.0$ for conifers. Except for V_{m25} and J_{m25}, all other leaf physiological parameters (see Table 1) are assumed to be invariant with canopy depth.

2.2.3. Wind-speed attenuation inside the canopy

Wind speed influences leaf energy balance by affecting leaf-boundary layer conductance and air humidity at the leaf surface (Nikolov et al. 1995). FORFLUX predicts the horizontal wind speed $w(L)$ under LAI of L employing Albini's phenomenological model (Albini, 1981) as modified by Massman (1987), i.e.

$$w(L) = w_o\exp\left(-K_w \frac{L}{L_{tot}}\right)$$
(13)

where w_o is the measured wind speed at the canopy top (m/s) and K_w is an extinction coefficient. Data compiled by Massman (1987) suggest that K_w varies as a function of total stand LAI according to the formula:

$$K_w = 2.879[1 - \exp(-L_{tot})]$$

2.2.4. Canopy precipitation interception

Water loss due to canopy interception of rainfall (I, mm/h) is estimated as a function of canopy water storage capacity (S_c, mm), rainfall intensity (R_o, mm/h), and evaporative demand (E_o, mm/h) using the analytical model of Massman (1983), i.e.

$$I = \begin{cases} S_c\left[1 - 0.667\dfrac{E_o}{(1-p)R_o}\right] + E_o & \text{if } E_o < (1-p)R_o \\ (1-p)R_o & \text{if } E_o \geqslant (1-p)R_o \end{cases}$$
(14)

Here, p is a throughfall coefficient, which defines the fraction of total rainfall reaching the ground without striking the canopy. Throughfall depends on the amount and distribution of canopy gaps, and, therefore, stand LAI and foliage clumping. In FORFLUX, p is predicted by:

$$p = \exp(-0.18\Omega_{cl}L_{tot})$$

The canopy water storage capacity is assumed to be proportional to stand LAI, i.e. $S_c = cL_{tot}$ where $c = 0.1$ mm/LAI for broad leaved vegetation (Sellers et al. 1988) and $c = 0.15$ mm/LAI for conifers (Hancock and Crowther 1979). Evaporative demand (E_o) is the amount of water that could be released to the atmosphere from a completely wet canopy during a time step. It is computed from the analytical solution to the canopy energy balance equation (see, Nikolov et al., 1995).

The photosynthesis of wet foliage at depth L is estimated by the LEAFC3 module assuming that evaporation completely suppresses transpiration, and wetness does not adversely impact the CO_2 assimilation capacity of leaves. The fraction of foliage area that remains wet during a time step (δ_{wet}) is computed following Dickinson et al. (1993).

2.2.5. Scaling leaf responses to the canopy level

Canopy evapotranspiration and net photosynthesis are computed by numerical integration of the LEAFC3 model over stand LAI. The canopy is vertically divided

into discrete layers. Layer thickness (ΔL) is defined in terms of LAI. It is adjustable, but has a default value of 0.4 $m^2 \; m^{-2}$, For each layer, the amount of sunlit LAI (L_{sun}) is estimated from the absorbed direct radiation by that layer and the beam extinction coefficient K (Monteith and Unsworth 1990, pp. 73-74), i.e.

$$L_{sun} = \frac{Q^{\downarrow}(L) - Q^{\downarrow}(L + \Delta L)}{K\Omega_{cl}} \qquad (15)$$

where $Q^{\downarrow}(X)$ is the fraction of direct beam at canopy depth X. The shaded LAI in a layer is computed as $L_{shad} = \Delta L - L_{sun}$.

Fluxes of absorbed radiation in the visible, near-infrared and thermal bands are separately estimated for sunlit and shaded foliage employing the radiative transfer model described above. Sunlit leaves are allowed to absorb both direct and diffuse radiation while shaded foliage only receives diffuse illumination. Finally, the LEAFC3 model is run for each foliage illumination class using appropriate values of leaf photosynthetic capacity and wind speed for that layer. Eventually, a canopy flux (F_c) is estimated as a sum of the corresponding fluxes from sunlit and shaded foliage in all layers.

The canopy integration scheme employed by FOR-FLUX assumes zero vertical gradients of air temperature, water vapor, and CO_2 concentration inside the canopy space. This simplification is supported by recent findings that, due to an efficient turbulent transport, the within-canopy variation of scalar concentrations is typically too small to significantly influence leaf physiological responses (e.g. Finnigan and Raupach, 1987; Baldochi, 1993). Micrometeorological studies also suggest that gradients of light and momentum are the most important. Ignoring the small effect of stand aerodynamic resistance on CO_2 and H_2O fluxes greatly simplifies the mathematical representation of canopy processes by avoiding conceptual and numerical problems associated with first- and second-order closure methods, and Lagrangian models (Massman and Grantz, 1995). However, canopy aerodynamic resistance is accounted for in predicting ozone deposition (see below).

2.2.6. Ozone deposition and plant ozone uptake

The FORFLUX model predicts total ozone deposition (F_{O3}) as a sum of three fluxes (Zeller and Nikolov, 2000), i.e. plant ozone uptake via leaf stomata, ozone deposition to non-transpiring plant surfaces, and ozone flux absorbed by the ground (i.e. soil or snow surface). Each component flux is a function of ambient ozone concentration and corresponding conductances and resistances along the pathway. These include the integrated foliage canopy conductance to ozone (g_{cs}, m s^{-1}), i.e. the sum in parallel of stomatal and leaf boundary-

layer conductances of all leaves; the plant surfacial (or cuticular) conductance to ozone deposition g_{ct} (m/s), and the above- and within-canopy aerodynamic resistances, r_a and r_u respectively; the soil boundary-layer resistance (r_{bs}), and the intrinsic soil resistance (r_{is}). The canopy conductance (g_{cs}) is the most influential one on the ozone flux among all resistances. It is estimated by integrating individual leaf ozone conductances (g_{lt}) for each canopy layer over the total stand LAI, i.e.

$$g_{cs} = \int_0^{L_i} g_{lt} \, dL \qquad (16)$$

where g_{lt} is calculated from the leaf stomatal (g_{sv}) and boundary-layer (g_{bv}) conductance to water-vapor exchange using the formula:

$$g_{lt} = \frac{g_{sv} g_{bv}}{1.315 \; g_{sv} + 1.508 \; g_{bv}} \qquad (17)$$

Here, the constants are ratios of water vapor and ozone diffusivities in still air and in the leaf-boundary layer, respectively. These are derived from data presented by Massman (1998). Vapor conductances, on the other hand, are computed by the coupled leaf photosynthesis-transpiration module (LEAFC3) of the FORFLUX model (see discussion above).

Canopy aerodynamic resistance (r_a) is estimated using an empirical equation derived from observations of vertical wind speed fluctuations above a subalpine ecosystem (Zeller and Nikolov, 2000):

$$r_a = \frac{19}{U^{1.35}} \qquad (18)$$

where U is the measured horizontal wind speed (m/s) above canopy. The plant surfacial conductance is estimated as a function of stand LAI, i.e. $g_{ct} = 0.5 \times 10^{-5} \, L_t$ (m s^{-1}) based on data by Kerstiens and Lendzian (1989) and Massman and Grantz (1995). The within-canopy aerodynamic resistance (r_u) is computed as a function of LAI and above-canopy wind speed, i.e.:

$$r_u = \frac{25 \; L_t}{0.065 \; U} \qquad (19)$$

The surface boundary-layer resistance to ozone is computed based on the ground boundary-layer conductance to water vapor ($g_{bs,v}$ m/s) using the formula

$$r_{bs} = \frac{1.37}{g_{bs.v}} \qquad (20)$$

where $g_{bs,v}$ is computed by the ground evaporation module of the FORFLUX model. This module solves exactly the surface energy balance equation while accounting for atmospheric stability effects on the ground boundary-layer conductance. The constant 1.37 is a ratio of molecular diffusivities of ozone and water vapor assumed in the surface boundary layer (Nikolov et al., 1995).

The intrinsic soil resistance to ozone exchange is considered to be constant over time. Based on information on soil resistances to ozone deposition gathered by Turner et al. (1974) and van Pul (1992), it is assumed $r_{is} = 410$ s m^{-1} for bare soil. In the presence of a snow pack, r_{is} is set to 6000 s m^{-1} as suggested by measurements of Zeller and Hehn (1995).

2.2.7. Above-ground woody respiration

The CO_2 flux originating from above-ground sapwood biomass is modeled using the functional approach of McCree (1970) and Amthor (1986). The total respiratory flux is partitioned into a maintenance and growth component.

Above-ground woody maintenance respiration ($R_{m,s}$, μmol m^{-2} s^{-1}) is assumed to be linearly related to the nitrogen content of living tissue (Ryan, 1991, 1995), and varies exponentially with air temperature (Amthor, 1984, 1986), i.e.

$$R_{m,s} = 0.2103 \ N_s \ Q_{10}^{0.1 \ (T_{lag3h} - 20)} \tag{21}$$

In this equation, N_s is the nitrogen content of the above-ground *sapwood* biomass (g m^{-2}), Q_{10} is the relative change of respiration rate per 10 °C temperature increase, and T_{lag3h} is ambient temperature (°C) lagged by three hours (Ryan et al., 1995). For unfertilized natural stands, N_s typically ranges between 1 and 13 g m^{-2} (Kimins et al., 1985). The Q_{10} values are reported to vary from 1.5 to 2.8 with a mean of about 2.2 (Ryan, 1991). Hagihara and Hozumi (1991) found that Q_{10} declines linearly with increasing mean monthly temperature. This acclimation response has been is included in the FORFLUX model, i.e.

$$Q_{10} = \begin{cases} 3.25 - 0.077 \ T_{7days} & \text{if} \quad T_{7days} \geqslant 0° \\ C3.25 & \text{if} \quad T_{7days} < 0°C \end{cases} \tag{22}$$

where T_{7days} is the mean daily temperature of the past seven days. Both T_{7days} and Q_{10} are updated daily in the model.

The CO_2 flux from above-ground woody biomass due to construction of new tissue ($R_{g,s}$, μmol m^{-2} s^{-1}) is assumed to be constant during a day and proportional to the net carbon gain of vegetation in the previous day, i.e.

$$R_{g,s} = f_g \ \delta_a \frac{(P'_c - R'_{m,s} - R'_{m,r})}{86.4} \tag{23}$$

where P'_c is the 24-h integrated canopy net photosynthesis (mmol m^{-2} d^{-1}), $R'_{m,r}$ and $R'_{m,s}$ are the cumulative daily maintenance respiratory fluxes (mmol m^{-2} d^{-1}) from roots and above-ground woody biomass, respectively, δ_a is the fraction of whole-plant growth allocated

above ground, and f_g is the construction cost (mol/mol). The factor 86.4 converts flux units of mmol m^{-2} d^{-1} to μmol m^{-2} s^{-1}. The carbon allocation coefficient (δ_a) depends on species physiology, tree age, and growth conditions (e.g. Cannell, 1985; Cannell and Dewar, 1994; Friend et al., 1994). This coefficient typically varies between 0.34 and 0.80 (e.g. Cannell, 1985). In the FORFLUX model, δ_a is defined as a system-specific input parameter. The whole-plant construction cost is rather consistent among tree species, and is treated as a constant in FORFLUX, i.e. $f_g = 0.2$ (Ryan, 1991).

The root maintenance respiration ($R'_{m,r}$) in Eq. (23) is estimated from the daily integral of root total respiration ($R'_{r,t}$) assuming roots have the same construction cost as the above-ground biomass, i.e.

$$R'_{m,r} = \frac{R'_{r,t} - f_g(1 - \delta_a)(P'_c - R'_{m,s})}{1 - f_g(1 - \delta_a)} \tag{24}$$

where $R'_{r,t}$ is computed as a site-specific fraction of the total CO_2 efflux from soil (Bowden et al., 1992; Nadelhoffer and Raich, 1992). The total above-ground woody respiration is the sum of $R_{m,s}$ and $R_{g,s}$.

2.2.8. Seasonal phenological variation of stand leaf area index

The physiological mechanisms of tree phenology are currently not well understood. Hence, existing models of plant phonological response are all empirical in nature (e.g. Cannel, 1990; Hunter and Lechowicz, 1992; Kramer, 1994; Hänninen, 1995). At present, FORFLUX only simulates foliage phenological dynamics of deciduous tree species. Evergreen vegetation is assumed to maintain a constant LAI throughout the year.

Seasonal LAI variation of deciduous stands is modeled using a four-stage approach. During autumn and winter, the canopy is assumed to be leafless. In spring, the date of budburst is predicted employing the parallel chill model of Murray et al. (1989). It based on the empirical observation that temperate tree species need certain amount of chilling for dormancy release. The heat sum required for the onset of leaf growth in spring is assumed to decline exponentially with the amount of chilling experienced during previous winter and autumn, i.e.

$$T_{cr} = a_{ph} + b_{ph}\exp(-r_{ph}D_c) \tag{25}$$

Here T_{cr} is the thermal time to budburst (i.e. the cumulative sum of mean daily temperatures above 5 °C from January 1), D_c is the number of chill days (i.e. days with mean daily temperature of 5 °C or less) from November 1, a_{ph}, b_{ph}, and r_{ph} are species-dependent constants (see Murray et al. 1989). Leaf growth commences when the heat sum accumulated from January 1 becomes equal to or greater than T_{cr}.

Foliage expansion from the onset of growth to full leaf development is computed daily as:

$$L_{t,j} = L_{t,j-1} + \Delta L \tag{26}$$

where L_t is current canopy LAI and $\ddot{A}L$ is the LAI growth from day *j*-1 to *j*. The daily LAI increment is modeled as a logistic function of mean daily temperature ($T_{a,j-1}$) on day *j*-1 (Shaykewich, 1995):

$$\Delta L = \frac{\Delta l_{\max}}{1 + \exp[A_{ex} - B_{ex}T_{a,j-1}]}\left(1 - \frac{L_{t,j-1}}{L_{\max}}\right) \tag{27}$$

in which $\Delta l_{\max}$ is a species-specific maximum foliage expansion rate (m² m⁻² d⁻¹), $L_{\max}$ is the LAI of the fully expanded canopy, and A_{ex} and B_{ex} are species-specific parameters. Data compiled by Shaykewich (1995) suggest that, across a range of species, $\Delta l_{\max} = 0.61$, $A_{ex} = 7.1$, and $B_{ex} = 0.4$.

The date of growth cessation in autumn is predicted using the joint factor model by Koski and Selkäinaho (1982) and Koski and Sievänen (1985). It assumes that the onset of leaf fall is triggered by a species-specific combination of increasing night length and a temperature sum (Hänninen et al. 1990).

2.3. Soil processes

The FORFLUX soil module simulates the temperature and moisture dynamics of soils, soil-surface evaporation, and CO_2 efflux from soil due to root and microbial respiration.

2.3.1. Water and heat transport in soil

Heat flow along with infiltration and redistribution of water are key physical processes in soils, which control important aspects of the ecosystem function such as water and nutrient uptake by plants, and organic matter decomposition. Predicting field-averaged transport of water and heat in soils requires stochastic (i.e. spatially distributed) approaches due to immense variation of soil hydraulic properties at the field scale and the extreme non-linearity of the flow process. This understanding has been adopted here. The FORFLUX soil model has two parts: a module that simulates the one-dimensional (vertical) flow of water and heat in a homogeneous soil column, and an algorithm that employs observed probability distributions of soil hydraulic properties to characterize field spatial heterogeneity in terms of a number of independent soil columns with different hydraulic characteristics and the percent area occupied by them. At every time step, the flow model is run for numerous individual columns. The output from these simulations is averaged weighted by the area represented by each column to yield mean soil water and heat fluxes at the ecosystem scale.

The homogeneous case of mass and energy transport in soil is modeled by combining Darcy's law with the continuity (mass-conserving) equation. This yields two one-dimensional partial differential equations containing derivatives of the dependent variables, i.e. soil temperature and volumetric moisture, with respect to time and space.

The vertical unsaturated flow of water in soils is described by the pressure-based form of the Richards' equation (Hillel, 1982; Feddes et al., 1988):

$$C_\theta \frac{\partial h_s}{\partial t} = \frac{\partial}{\partial z}\left[K(h_s)\left(\frac{\partial h_s}{\partial z} - \gamma\right)\right] + S(z;t) \tag{28}$$

where $C_\theta \equiv \partial\theta/\partial h_s$ is the specific moisture capacity (m⁻¹), θ is the volumetric moisture content (m³ m⁻³), *t* is time (*h*), *z* is the vertical soil depth (m), h_s is the pressure head (m), $K(h_s)$ is the hydraulic conductivity (m h⁻¹) at head h_s, ã is the cosine of the terrain slope, and $S(z;t)$ is the source/sink term (m³ m⁻³ h⁻¹). Since FORFLUX does not consider lateral water transport, $S(z;t)$ reduces to a sink term representing the root water uptake.

Solving the Richards' equation requires knowledge of the moisture retention curve $\theta(h_s)$ and the unsaturated conductivity curve $K(h_s)$. Both relationships are highly non-linear and their shapes vary greatly with soil physical properties. FORFLUX computes $\theta(h_s)$ using a function proposed by van Genuchten (1980):

$$\theta(h) = \frac{\theta_s - \theta_r}{1 + (-\alpha h_s)^n} + \theta_r \tag{29}$$

where θ_s is the soil moisture content at saturation (m³ m⁻³), θ_r is the residual (irreducible) soil moisture (m³ m⁻³) while α and *n* are empirical parameters related to soil physical properties. The dependence of hydraulic conductivity on pressure head is modeled after Gardner (1958), i.e.

$$K(h_s) = 0.01\frac{K_{sat}}{1 + (-b_k h_s)^{\lambda_k}} \tag{30}$$

where K_{sat} is the saturated hydraulic conductivity (cm h⁻¹), and b_k and λ_k are soil-specific parameters. Differentiating Eq. (29) with respect to h_s yields an expression for the specific moisture capacity in Eq. (28), i.e.

$$C_\theta \equiv \frac{\partial\theta}{\partial h_s} = -(\theta_s - \theta_r)\frac{\alpha^n n h_s^{n-1}}{[1 + (-\alpha h_s)^n]^2} \tag{31}$$

The functional dependence of h_s on soil moisture is obtained by inverting Eq. (29), i.e.

$$h_s(\theta) = -\frac{1}{\alpha}\left[\frac{\theta_s - \theta_r}{\theta - \theta_r} - 1\right]^{\frac{1}{n}} \tag{32}$$

Several pedo-transfer functions have been proposed to estimate parameters θ_s, θ_r, α, n, K_{sat}, b_k and λ_k using easily measurable soil physical properties (e.g. Clapp and Horn-berger, 1978; Gupta and Larson, 1979; De Jong et al., 1983; Cosby et al., 1984; Saxton et al., 1986; Vereecken et al., 1989, 1990). The FORFLUX model employs pedo-transfer functions developed by Vereecken et al. (1989, 1990), which have been found to produce satisfactory results over a wide range of soil types and soil matrix potentials (Kern, 1995). Vereecken and colleagues used data from 42 Belgian soil types to relate the above pedo-parameters to soil bulk density and soil texture defined in terms of percent content of sand, clay, silt and organic carbon.

A variety of models have been proposed for estimating the root sink term $S(z;t)$ in Eq. (28) above (Molz, 1981a). FORFLUX computes $S(z;t)$ using a modified version of the formulation proposed by Molz (1981b). At any given soil depth, root water uptake is proportional to canopy transpiration and depends on root length density, the resistance to water flow from soil to roots, and the water-potential gradient between roots and soil, i.e.

$$S(z; t) = -\frac{E(t)}{\rho_w}\,\frac{L_r(z)\Delta h\ g_r(z; t)}{\int_0^{z_r} L_r(z)\Delta h\ g_r(z; t)dz} \tag{33}$$

In this equation, $E(t)$ is the canopy transpiration (kg m^{-2} h^{-1}) at time t, ρ_w is the density of liquid water ($\rho_w = 1000$ kg m^{-3}), $L_r(z)$ is the root length density at depth z normalized by the root density near the soil surface, $g_r(z;t)$ is the relative conductance to water flow in the soil–root interface at depth z and time t ($0 \leqslant g_r \leqslant 1$), Δh is the pressure-head gradient between plant roots and the soil, and Z_r is the plant rooting depth (m) defined as the soil depth which contains 97% of the total root length.

We modified the Molz's equation for $S(z;t)$ by adding a root conductance term. Studies on root water extraction suggest that the greatest resistance to water flow occurs at the soil–root interface (Molz, 1981a; Bristow et al., 1984). This resistance is caused by the loss of physical contact between roots and the soil matrix as moisture declines. FORFLUX simulates $g_r(z;t)$ as a combined function of soil moisture and temperature, i.e.

$$g_r(z; t) = \frac{f_M + f_T - \sqrt{(f_M + f_T)^2 - 4\omega_g f_M f_T}}{2\omega_g} \tag{34}$$

where f_M and f_T are non-dimensional factors defining the effect of moisture and temperature conditions,

respectively, at depth z and time t, and $\omega_g = 0.99$ is a convexity coefficient which determines the smoothness of the transition between moisture and temperature limitations on root resistance. Bristow et al. (1984) found that, over a range of soil textures and water potentials, the interfacial resistance is uniquely related to the relative soil saturation (θ/θ_s). Based on their analysis, f_M is estimated as

$$f_M(z; t) = \frac{1}{1 + a_r\exp\left[-b_r\left(\dfrac{\theta(z; t) - \theta_r}{\theta_s - \theta_r} - c_r\right)\right]} \tag{35}$$

where a_r, b_r and c_r are species-specific parameters having default values of 2, 30, and 0.25, respectively. The temperature factor is calculated as

$$f_T(z; t) = \frac{1}{1 + \exp\left[4.701\left(1 - \dfrac{T_{sl}(z; t)}{T_{cr}}\right)\right]} \tag{36}$$

where $T_{sl}(z;t)$ is soil temperature ($^\circ$C) at depth z and time t, and T_{cr} is a species-dependent parameter defining the soil temperature ($^\circ$C) at which root conductance is reduced by 50%. For most temperate tree species, $2\ ^\circ\text{C} < T_{cr} < 8\ ^\circ\text{C}$.

Unlike plant root biomass, which has been found to decline exponentially with soil depth (e.g. Gale and Grigal, 1986), root length density (m m^{-3}) tends to follow a linear vertical trend (e.g. Carbon et al., 1980). In this model, $L_r(z)$ is given by

$$L_r(z) = \begin{cases} 1 - 0.85\dfrac{z}{Z_r} & \text{if} \quad z \leqslant Z_r \\ 0.0 & \text{if} \quad z > Z_r \end{cases} \tag{37}$$

The pressure-head gradient (Δh) in the sink-term equation is assumed to be constant and equal to 0.35 m. This is in accordance with the notion that, in drying soils, the increase of interfacial resistance cannot be compensated for by an increased pressure head gradient.

The temperature dynamics of the soil profile is described by the partial differential equation (Hillel, 1982; Campbell, 1985):

$$C_h(\theta)\frac{\partial T}{\partial t} = \frac{\partial}{\partial z}\left[\lambda_T(\theta)\frac{\partial T}{\partial z}\right] \tag{38}$$

where T is soil temperature ($^\circ$C), $C_h(\theta)$ is volumetric heat capacity of soil (J m^{-3} K^{-1}), $\lambda_T(\theta)$ is the apparent thermal conductivity of soil (W m^{-1} K^{-1}), t is time (s), and z is vertical depth (m). Soil heat capacity increases linearly with bulk density, volumetric moisture, and volumetric fraction of rocks f_r (Campbell, 1985), i.e.

$$C_h(\theta) = \{0.869[(1-f_r)\rho_{bs} + 2.65f_r] + 4.186(1-f_r)\theta\}10^6 \tag{39}$$

All particles with a diameter greater than 2 mm are classified as *rocks*. In Eq. (39), the constant 2.65 is the density of soil clay minerals and rocks (g cm^{-3}) while 4.186 the specific heat of water (J g^{-1} K^{-1}). Soil thermal conductivity is estimated using an empirical formula proposed by Cass et al. (1984) and Campbell (1985), which accounts for the combined effect of sensible and latent heat transport on total conductivity, i.e.

$$\lambda_T(\theta) = A_{TK} + B_{TK}\theta(1-f_r)$$
$$- (A_{TK} - D_{TK})\exp\{-[C_{TK}\theta(1-f_r)]^4\} \tag{40}$$

where coefficients A_{TK}, B_{TK}, C_{TK} and D_{TK} depend on total porosity (θ_s), rock content, and percent clay of soil (see Campbell, 1985 for details).

Solving diffusion Eqs. (28) and (38) requires appropriate boundary conditions. At the soil-atmosphere interface, fluxes of water and heat are coupled through the surface energy balance. Two types of upper boundary conditions are simulated in the model for water flow: (1) If, during a time step, a rainfall or snowmelt event delivers a liquid water flux into the soil which exceeds soil evaporation (E_s, mm/s), the surface conditions are specified in terms of zero pressure head; (2) In the absence of rainfall or snowmelt, water is transported as vapor across the soil-atmosphere boundary. Unlike liquid water flow, which is mainly controlled by matric pressure gradients in soil, vapor flux is primarily driven by vertical differences in vapor pressure and temperature within the upper soil column. At the very surface, vapor flux is coupled with other soil heat fluxes via the standard energy balance equation. This equation is solved analytically using the method of Nikolov *et al.* (1995) while accounting for the surface aerodynamic resistance (as controlled by atmospheric stability, e.g. Brutsaert, 1982) and the intrinsic soil conductance to water vapor (Kondo et al., 1990; Griend and Owe, 1994).

The model simulates two types of lower boundary conditions for water transport and one for heat flow. If a water table is present at the bottom of the soil slab (which is defined in the input file), a Dirichlet condition is prescribed assuming that the soil is always saturated at the bottom and pressure head is held constant. In the absence of a water table, a Neumann condition of free drainage applies. In this case, a zero gradient of pressure head at the lower soil boundary is assumed. The temperature at the bottom of the soil column is assumed to exhibit no diurnal fluctuations, and is updated once per day using a closed-form solution of the heat flow equation (see Campbell, 1985).

The partial differential Eqs. (28) and (38) are solved numerically using a semi-implicit finite-difference method. The solution to water flow employs a non-iterative mass-conservative scheme called flux-updating conjugate gradient algorithm proposed by Kirkland et al. (1992). The spatial discretization utilizes irregular vertical grid with a mesh-cell size geometrically increasing with depth. The thickness of the topsoil layer is 0.2 cm, and the maximum number of layers allowed is 20. This numerical scheme ensures a high spatial resolution near the top of the soil column where gradients of temperature and moisture are the steepest while using a small number of layers. This improves both the accuracy and computational efficiency of the algorithm. The solution is advanced hourly in time.

2.3.2. CO_2 evolution from soil

FORFLUX implements a simple bulk parameterization approach to predict soil CO_2 efflux, which only considers the effect of soil moisture, temperature and clay content (Cl) on the net CO_2 release. The simplicity of this method ensures easy applicability of the model to a wide variety of ecosystems. The CO_2 evolution from soil (F_{CO2}, μmol m^{-2} s^{-1}) is estimated as:

$$F_{CO2} = F_{max}\frac{f_M + f_T - \sqrt{(f_M + f_T)^2 - 4\omega f_M f_T}}{2\omega}$$
$$\times (1 - 0.0065 \ Cl) \tag{41}$$

where F_{max} is the rate of soil respiration (μmol m^{-2} s^{-1}) under optimum temperature and moisture conditions, f_T and f_M are non-dimensional factors quantifying the limitations of temperature and moisture, respectively, on the CO_2 efflux, and $\omega = 0.985$ is a convexity coefficient defining the smoothness of the transition between f_T and f_M.

The temperature factor is computed after Kirschbaum (1995) who derived an expression for f_T based on soil respiration data from 11 studies worldwide, i.e.

$$f_T = \exp\left[-3.764 + 0.204 \ T\left(1 - 0.5\frac{T}{T_{op}}\right)\right] \tag{42}$$

where T is the soil temperature (°C) at 10 cm depth, and T_{op} is the optimum temperature for CO_2 evolution ($T_{op} = 36.9$ °C). This equation implies a variable Q_{10}. The effect of volumetric moisture on soil respiration is described based on measurements and models by Schlentner and Van Cleve (1984) and Grant and Rochette (1994), i.e.

$$f_M = \begin{cases} \dfrac{1}{1 + \exp[3.0 - 14.0 \ s]} & \text{if} \quad 0 \leqslant s \leqslant 0.74 \\ \dfrac{1}{1 + \exp[3.0 - 76.0(1-s)]} & \text{if} \quad 0.74 < s \leqslant 1.0 \end{cases} \tag{43}$$

where s is the relative moisture saturation at 14 cm depth, $s = (\theta - \theta_r)/(\theta_s - \theta_r)$.

Data from hardwood forests around the world compiled by Peterjohn et al. (1994) suggest that, on average, $F_{max} = 17$ μmol m^{-2} s^{-1}. FORFLUX uses this value whenever no maximum rate of soil CO_2 flux is specified for a particular ecosystem. Clay content is assumed to impact negatively soil respiration in accordance with results from a C isotope study by Amato and Ladd (1992). The CO_2 evolution at the field scale is predicted as an area-weighted average of the CO_2 fluxes from many individual soil columns.

2.4. Root–shoot communication: coupling soil fluxes to canopy processes

Canopy exchange processes are physically linked to soil heat- and water-transport mechanisms via the stem sap flow. Sap flow is the pipeline that transports water from deeper soil layers into the atmosphere while communicating moisture and temperature conditions of the rhizosphere to the photosynthetic apparatus of leaves in the canopy.

There is a growing body of evidence that hydraulic signals such as tissue water potential alone cannot explain leaf stomatal response to soil drought and freezing. Apparently, roots release a hormonal message which, in many cases, seems to be even more important than the hydraulic message in regulating stomatal conductance, plant growth and root-shoot carbon allocation (e.g. Zhang and Davies, 1989; Gowing et al., 1993; Munns and Sharp, 1993, Tardieu et al., 1993, Tardieu and Davies, 1993a; Bertrand et al., 1994; Jackson et al., 1995). This message is currently identified with the concentration of abscisic acid in the xylem sap ([ABA], μmol m^{-3}). Tardiue and co-workers found that the sensitivity of stomatal conductance to [ABA] increases exponentially with falling leaf water potential (Tardieu et al., 1993; Tardieu and Davies, 1993a,b), i.e.

$$g_s = \exp(-[ABA]\beta\exp(\delta\psi_l))$$

where g_s is the relative stomatal conductance to water vapor, ψ_l is leaf water potential (-MPa), and β and δ are empirical parameters so that $\beta > 0$ and $\delta < 0$. The xylem ABA concentration depends linearly on root water potential ψ_r (-MPa) and is inversely related to transpirational water flux E through the plant (which is assumed to dilute the hormonal message).

The FORFLUX model implements a root-shoot communication algorithm, which is based on the above approach by Tardieu et al. (1993). The root signal (υ'_r) emitted to leaf stomata from a soil column p at time t is an integral of the signals originating from all depths (layers) of that column, i.e.

$$\vartheta_r(p; t) =$$
$$\int_0^{Z_r} S_{rel} \exp\left\{\left[h_s - \frac{0.35}{g_r(p; z; t)}\right]\frac{A_r}{E + C_r}\exp[-B_r h_s]\right\}dz$$
(44)

where E is the canopy transpiration rate, $g_r(p;z;t)$ is the root interfacial conductance at depth z and time t estimated as described above, A_r, B_r, and C_r are species-specific parameters, $h_s(p;z;t)$ is the soil water pressure head, Z_r is the rooting depth, and $S_{rel}(p;z;t)$ is a weighting factor specifying the relative root water uptake at depth z computed as

$$S_{rel}(p; z; t) = \frac{L_r(z)\Delta h \; g_r(p; z; t)}{\int_0^{z_r} L_r(z)\Delta h \; g_r(p; z; t)dz}$$
(45)

If E is expressed in *mm/h* and h_s is in *m*, then typically $11 \times 10^{-6} \leqslant A_r \leqslant 65 \times 10^{-6}$, $B_r \approx 0.026$, and $C_r \approx 0.014$.

The field averaged root signal ($\tilde{O}_r$) is computed as a weighted sum of the signals from all columns characterizing the soil heterogeneity at a particular site, i.e.

$$Y_r(t) = \sum_{p=1}^{N_p} \vartheta_r(p; t)P(p)$$
(46)

where $P(p)$ is the probability of occurrence of soil column p, and N is the number of simulated columns.

Since $0 \leqslant Y_r \leqslant 1$, the averaged root signal is passed as a non-dimensional multiplier to the LEAFC3 module to constrain stomatal conductance of all leaves in the canopy at a given time step. Specifically, $\tilde{O}_r$ is incorporated in the Ball–Berry stomatal model, i.e.

$$g_{sv} = Y_r \; mA_n \frac{h_b}{c_b} + b_{sv}$$
(47)

where parameters m, h_b and c_b are as described by Nikolov et al. (1995, pp. 208–209).

2.5. Snow pack model

This module simulates the dynamics of snow accumulation and snowmelt on the ground. Precipitation is partitioned into rain- and snow-fall based on ambient temperature (Wigmosta et al., 1994). If $T_a < -1.1$ °C, precipitation is assumed to be exclusively in the form of snow. When $T_a > 3.3$ °C, all precipitation falls as rain. Between these temperature thresholds, precipitation is modeled as a mix of rain and snow.

Since the model assumes that snow interception by the canopy is negligibly small, all snowfall is added to the ground storage. The snowpack is depleted through sublimation and melting. Both processes are assumed to occur at the snow–atmosphere interface and be driven

by the snowpack energy balance (Male and Gray, 1981), i.e.

$$Q_m = R_{is} + G_{sn} + Q_p - H_s - L_s$$

$$E_{sn} - \varepsilon\sigma(T_s + 273.16)^4 - \frac{d\ U_s}{d\ t} \tag{48}$$

where Q_m is the energy flux available for melt, R_{is} is the total radiation absorbed by the snow-pack, G_{sn} is the heat flux from the snow–ground interface, Q_p is the energy advected by precipitation, H_s and L_sE_{sn} are the fluxes of sensible and latent heat, respectively, at the snow–atmosphere interface (E_{sn} is sublimation in mm/s while L_s is the latent heat of sublimation in J/kg), T_s is the snow surface temperature, and dU_s/dt is the rate of change of energy stored in the snowpack (the units of all energy fluxes are W m^{-2})

The snowpack radiation absorption is computed as a function of incident visible, near-infrared and thermal irradiances and corresponding spectral albedos of snow:

$$R_{is} = (1 - \alpha_{sn,vis})I^{\downarrow}_{vis} + (1 - \alpha_{sn,nir})I^{\downarrow}_{nir} + I^{\downarrow}_{lw} \tag{49}$$

Snow spectral albedos in the visible and near-infrared wavelength (i.e. $\alpha_{sn,vis}$ and $\alpha_{sn,nir}$) are estimated using the physical model of Marshall (1989), which accounts for effects of snow grain radius, impurity content, snowpack depth, solar zenith angle and cloud cover. Snow depth and soot concentration primarily influence $\alpha_{sn,vis}$ while grain size and solar zenith angle mainly affect $\alpha_{sn,nir}$. An accurate prediction of snow spectral reflectances is important due their large seasonal variation, and strong impact on the surface energy balance. The ground heat flux is computes as

$$G_s = \lambda_{sn}\frac{(T_b - T_s)}{Z_{sn}} \tag{50}$$

where λ_{sn} is the average snowpack thermal conductivity (W m^{-1} K^{-1}), T_b is the temperature at the snow-ground interface (°C) , and Z_{sn} is the snow depth (m). The FORFLUX model assumes a fixed value for snow thermal conductivity, i.e. $\lambda_{sn} = 0.2$ W m^{-1} K^{-1}.

The other energy fluxes in Eq. (47) are estimated as follows:

$$Q_p = \rho_w C_w(T_a - T_s)(P_r + 0.5\ P_s) \tag{51}$$

$$H_s = \rho c_p(T_s - T_a)g_b \tag{52}$$

$$E_s = 0.622\frac{\rho}{P_a}[e_s(T_s) - e_a]g_b \tag{53}$$

$$U_s = Z_{sn}\rho_s C_s\frac{(T_s + T_b)}{2} \tag{54}$$

In these equation, ρ_w is the density of liquid water (1000 kg m^{-3}), C_w is the heat capacity of water (4186 J kg^{-1} K^{-1}), ρ_s is the density of snow (310–420 kg m^{-3}), C_s is the heat capacity of ice ($C_s = 0.5C_w$), and $[e_s(T_s)$–$e_a]$ is the vapor pressure gradient between snow surface and the atmosphere. The snow boundary-layer conductance (g_b) is estimated using the Mobin–Obikov theory and assuming a roughness length of 0.001 m.

A distinctive characteristic of the snowpack energy balance (compared to other surfaces) is that the surface temperature of snow cannot exceed 0 °C regardless of the amount of external energy input. This is so because the latent heat of fusion of ice is about 10 times smaller that the latent heat of sublimation. As a result, excess energy always goes into melting of snow rather than into sublimation. This needs be considered when solving the energy balance Eq. (47). First, the right side of the equation is evaluated using $T_s = 0$ °C and $e_s(T_s) = 602.73$ Pa. If $Q_m > 0$, a snowmelt is assumed to occur and the estimates of fluxes of latent and sensible heat are accepted. The amount of melt water (M, mm/s) is then computed as

$$M = \frac{Q_m}{\rho_w h_f} \tag{55}$$

where h_f is the latent heat of fusion (333.5×10^3 J/kg). The melt water is allowed to percolate through the snowpack and drain into the soil. The time lag from the onset of snowmelt until drainage commences is modeled using the empirical method of Conway and Benedict (1994). If $Q_m < 0$, then the snowmelt is zero, and the energy balance equation is solved for the snow-surface temperature using an analytical techniques similar to one employed by Nikolov et al. (1995). Liquid water is assumed to refreeze in the snowpack and drainage to stop at a given time step, if the average snowpack temperature ($T_s + T_b$)/2 plummets below −1 °C.

3. Conclusion

The FORFLUX model presents a new comprehensive biophysical approach towards studying, predicting and analyzing pollution deposition, the exchange of trace gases and energy between terrestrial ecosystems and the atmosphere. The model has been successfully verified against flux data measured over different ecosystems (e.g. Nikolov, 1997; Zeller and Nikolov, 2000; Amthor et al. 2001), and applied in climate change studies (Potter et al., 2001). A companion publication discusses FORFLUX simulations and applications to a high-altitude subalpine forest ecosystem in southern Wyoming (USA).

Acknowledgements

References

Aber, J.D., Federer, C.A., 1992. A generalized, lumped-parameter model of photosynthesis, evapotranspiration and net primary production in temperate and boreal forest ecosystems. Oecologia 92, 463–474.

Albini, F.A., 1981. A phenomenological model for wind speed and shear stress profiles in vegetation cover layers. J. App. Meteorol. 20, 1325–1335.

Amato, M., Ladd, J.N., 1992. Decomposition of ^{14}C- labelled glucose and legume material in soils: properties influencing the accumulation of organic residue C and microbial biomass C. Soil Biol. Biochem. 24 (5), 455–464.

Amthor, J.S., 1986. Evolution and applicability of a whole plant respiration model. J. Theoretical Biology 122, 473–490.

Amthor, J.S., Chen, J.M., Clein, J.S., Frolking, S.E., Goulden, M.L., Grant, R.F., Kimball, J.S., King, A.W., McGuire, A.D., Nikolov, N.T., Potter, C.S., Wang, S., Wofsy, S.C., 2001. Boreal forest CO_2 exchange and evapo-transpiration predicted by nine ecosystem process models: intermodel comparisons and relationships to field measurements. J. Geophys. Res. 106 (33), 623–633,648.

Amthor, J.S., 1984. The role of maintenance respiration in plant growth. Plant, Cell and Environ. 7, 561–569.

Baldocchi, D.D., 1993. Scaling water vapor and carbon dioxide exchange from leaves to a canopy: rules and tools. In: Eleringer, J.R., Field, C.B. (Eds.), Scaling Physiological Processes. Leaf to Globe. Academic Press, San Diego, pp. 77–116.

Bertrand, A., Robitaille, G., Nadeau, P., Boutin, R., 1994. Effects of soil freezing and drought sress on abscisic acid content of sugar maple sap and leaves. Tree Physiology 14, 413–425.

Bonnan, G.B., 1989a. A biophysical surface energy budget analysis of soil temperature in the boreal forests of interior Alaska. Water Resour. Res. 27, 767–781.

Bonnan, G.B., 1991b. Atmosphere-biosphere exchange of carbon dioxide in boreal forests. J. Geophys. Res. 96, 7301–7312.

Bowden, R., Nadelhoffer, K.J., Boone, R.D., Melillo, J.M., Garrison, J.B., 1992. Contributions of aboveground litter, belowground litter, and root respiration to total soil respiration in a temperate mixed hardwood forest. Can. J. For. Res. 23, 1402–1407.

Bristow, K.L., Campbell, G.S., Calissendorff, C., 1984. The effects of texture on the resistance to water movement within the rhizosphere. Soil Sci. Soc. Am. J. 48, 266–270.

Brooks, J.R., Flanagan, L.B., Varney, G.T., Ehleringer, J.R., 1997. Vertical gradients in photosynthetic gas exchange characteristics and refixation of respired CO_2 within boreal forest canopy. Tree Physiology 17, 1–12.

Brutsaert, W.H., 1982. Evaporation into the Atmosphere. Theory, History, and Applications. D. Reidel Publishing Company, Dordrecht.

Brutsaert, W.H., 1975. On a derivable formula for long-wave radiation from clear skies. Water Resources Research 11, 742–744.

Camillo, P., 1987. A canopy reflectance model based on an analytical solution to the multiple scattering equation. Remote Sensing of Environ. 23, 453–477.

Campbell, G.S., 1985. Soil Physics with Basics. Transport Models for Soil-Plant Systems. Elsevier Sci. Pub, Amsterdam.

Campbell, G.S., 1986. Extinction coefficient for radiation in plant canopies calculated using an ellipsoidal inclination angle distribution. Agric. For. Meteor. 36, 317–321.

Campbell, G.S., 1990. Derivation of an angle density function for canopies with ellipsoidal leaf angle distributions. Agric. For. Meteor. 49, 173–176.

Cannell, M.G.R., 1985. Dry matter partitioning in tree crops. In: Cannell, M.G.R., Jackson, J.E. (Eds.)., Attributes of Trees as Crop Plants, Institute of Terrestrial Ecology, pp. 160–193

Cannell, M.G.R., 1990. Modelling the phenology of trees. Silva Carelica 15, 11–27.

Cannell, M.G.R., Dewar, R.C., 1994. Carbon allocation in trees: a review of concepts and modelling. Adv. Ecol. Research 25, 50–104.

Carbon, B.A., Bartle, G.A., Murray, A.M., Macpherson, D.K., 1980. The distribution of root length, and the limits to flow of soil water to roots in a dry sclerophyll forest. Forest Sci. 26 (4), 656–664.

Cass, A., Campbell, G.S., Jones, T.L., 1984. Enhancement of thermal water vapor diffusion in soil. Soil Sci. Soc. Am. J. 48, 25–32.

Clapp, R.B., Hornberger, G.M., 1978. Empirical equations for some soil hydraulic properties. Water Resour. Res. 14, 601–604.

Conway, H., Benedict, R., 1994. Infiltration of water into snow. Water Resour. Res. 30 (3), 641–649.

Cosby, B.J., Hornberger, G.M., Clapp, R.B., Ginn, T.R., 1984. A statistical exploration of the relationship of soil moisture characteristics to the physical properies of soils. Water Res. Research 20 (6), 682–690.

De Jong, R., Campbell, C.A., Nicholaichuck, W., 1983. Water retention equations and their relationship to soil organic matter and particle size distributions for disturbed samples. Can. J. Soil Sci. 63, 291–302.

Dickinson, R. E., Handerson-Sellers, A. and Kennedy, P. J. 1993. Biosphere-Atmosphere Transfer Scheme (BATS) Version 1e as Coupled to the NCAR Community Climate Model. NCAR Technical Note NCAR/TN-387 + STR, NCAR Boulder, pp. 72.

Ellsworth, D.S., Reich, P.B., 1993. Canopy structure and vertical patterns of photosynthesis and related leaf traits in a deciduous forest. Oecologia 96, 169–178.

Feddes, R.A., Kabat, P., Van Bakel, P.J.T., Bronswijk, J.J.B., Halbertsma, J., 1988. Modelling soil water dynamics in the unsaturated zone—state of the art. J. Hydrology 100, 69–111.

Field, C., 1983. Allocating leaf nitrogen for maximization of carbon gain: leaf age as a control on the allocation program. Oecologia 56, 341–347.

Finnigan, J.J., Raupach, M.R., 1987. Transfer processes in plant canopies in relation to stomatal characteristics. In: Zeigler, E., Farquhar, G.D., Cowan, I.R. (Eds.), Stomatal Function. Standford University Press, Standford, pp. 385–430.

Friend, A.L., Coleman, M.D., Isebrands, J.G., 1994. Carbon allocation to root and shoot systems of woody plants. In: Davis, T.D., Hassig, B.E. (Eds.), Biology of Adventitious Root Formations. Plenum Press, New York, pp. 245–273.

Gale, M.R., Grigal, D.F., 1986. Vertical root distributions of northern tree species in relation to successional status. Can. J. For. Res. 17, 829–834.

Gardner, W.R., 1958. Some steady-state solotions of the unsaturated moisture flow equation with applications to evaporation from a water table. Soil Sci. 85, 228–232.

Gowing, D.J.G., Davies, W.J., Trejo, C.L., Jones, H.G., 1993. Xylem-transported chemical signals and the regulation of plant growth and physiology. Philos. Trans. R. Soc. London 314, 41–47.

Grant, R.F., Rochette, P., 1994. Soil microbial respiration at different water potentials and temperatures: Theory and mathematical modeling. Soil Sci. Soc. Am. J. 58, 1681–1690.

Griend, A.A., Owe, M., 1994. Bare soil surface resistance to evaporation by vapor diffusion under semiarid conditions. Water Resour. Res. 30 (2), 181–188.

Gupta, S.C., Larson, W.E., 1979. Estimating soil water retention characteristics from particle size distribution, organic matter content and bulk density. Water Resour. Res. 15, 1633–1635.

Hagihara, A., Hozumi, K., 1991. Respiration. In: Raghavendra, A.S. (Ed.), Physiology of Trees. John Wiley and Sons, New York, pp. 87–110.

Hancock, N.H., Crowther, J.M., 1979. A technique for the direct measurement of water storage on a forest canopy. J. Hydrology 41, 105–122.

Hänninen, H., 1995. Effects of climatic change on trees from cool and temperate regions: an ecophysiological approach to modelling of bud burst phenology. Can. J. Bot. 73, 183–199.

Hänninen, H., Häkkinen, R., Hari, P., Koski, V., 1990. Timing of growth cessation in relation to climatic adaptation of northern woody plants. Tree Phys. 6, 29–39.

Heitor, A., Biga, A.J., Rosa, R., 1991. Thermal radiation components of the energy budget at the ground. Agric. For. Meteor. 54, 29–48.

Handerson-Sellers, A., Pitman, A.J., 1992. Land-surface schemes for future climate models: specification, aggregation, and heterogeneity. J. Geophys. Res. 97, 2687–2696.

Hillel, D., 1982. Introduction to Soil Physics. Academic Press, Orlando.

Hirose, T., Werger, M.J.A., 1987. Maximizing daily canopy photosynthesis with respect to the leaf nitrogen allocation pattern in the canopy. Oecologia 72, 520–526.

Hirose, T., Werger, M.J.A., Pons, T.L., van Rheenen, J.W.A., 1988. Canopy structure and leaf nitrogen distribution in a stand of Lysimachia vulgaris L. as influenced by stand density. Oecologia 77, 145–150.

Hunter, A.F., Lechowicz, M.J., 1992. Predicting the timing of budburst in temperate trees. J. App. Ecol. 29, 597–604.

Jackson, G.E., Irvine, J., Grace, J., Khalil, A.A.M., 1995. Abscisic acid concentrations and fluxes in droughted conifer saplings. Plant, Cell and Environ 18, 13–22.

Jarvis, P.G., 1976. The interpretation of the variations in leaf water potential and stomatal conductance found in canopies in the field. Philos. Trans. Roy. Soc. London, Ser B 273, 593–610.

Kern, J.S., 1989. Evaluation of soil water retention models based on basic soil physical properies. Soil Sci. Soc. Am. J. 59, 1134–1141.

Kerstiens, G., Lendzian, K.J., 1989. Interactions between ozone and plant cuticles. I. Ozone deposition and permeability. New Physiologist 112, 13–19.

Kimins, J.P., Binkley, D., Chatarpaul, L. and de Catanzaro, J. 1985. Biogeochemistry of Temperate Forest Ecosystems: Literature and Dynamics of Biomass and Nutrients. Petawawa National Forestry Institute, Canadian Forestry Service.

Kirkland, M.R., Hills, R.G., Wierenga, P.J., 1992. Algorithms for solving Richards' equation for variably saturated soils. Water Resour. Res. 28 (8), 2049–2058.

Kirschbaum, M.U.F., 1995. The temperature dependence of soil organic matter decomposition, and the effect of global warming on soil organic storage. Soil Biol. Biochem. 27 (6), 753–760.

Kondo, J., Saigusa, N., Sato, T., 1990. A parameterization of evaporation from bare soil surfaces. J. App. Meteor. 29, 385–389.

Koski, V., Selkäinaho, J., 1982. Experiments on the joint effect of heat sum and photoperiod on seedlings of *Betula pendula*. Commun. Inst. For. Fenn. 105, 1–34.

Koski, V., Sievänen, R., 1985. Timing of growth cessation in relation to the variations in the growing season. In: Tigerstedt, P.M.A., Puttonen, P., Koski, V. (Eds.), Crop Physiology of Forest Trees. Helsinki University Press, Helsinki, pp. 167–193.

Kramer, K., 1994. Selecting a model to predict the onset of growth of Fagus sylvatica. J. App. Ecol. 31, 172–181.

Leuning, R., Cromer, R.N., Rance, S., 1991. Spatial distribution of foliar nitrogen and phosphorus in crowns of *Eucalyptus grandis*. Oecologia 88, 504–510.

Male, D.H., Gray, D.M., 1981. Snowcover ablation and runoff. In: Gray, D.M., Male, D.H. (Eds.), Handbook of Snow. Principles, Processes, Management & Use. Pergamon Press, Toronto, pp. 360–436.

Marks, D., Dozier, J., 1979. A clear-sky longwave radiation model for remote alpine areas. Archiv für Meteorologie. Geophysik und Bioklimatologie B-27, 159–187.

Marshall, S.E. 1989. A Physical Parameterization of Snow Albedo for Use in Climate Models. PhD dissertation, Department of Gegraphy, University of Colorado, pp. 190.

Massman, W.J., 1987. A comparative study of some mathematical models of the mean wind structure and aerodynamic drag of plant canoipies. Boundary-Layer Meteor. 40, 179–197.

Massman, W.J., 1983. The derivation and validation of a new model for the interception of rainfall by forests. Agric. Meteor. 28, 261–286.

Massman, W.J., 1998. A review of the molecular diffisivities of H_2O, CO_2, CH_4, CO, SO_2, NH_3, N_2O, NO, and NO_2 in air, O_2, and N_2, near STP. Atmos. Environ 32 (6), 1111–1127.

Massman, W.J., Drantz, D.A., 1995. Estimating canopy conductance to ozone uptake from observations of evapotranspiration at the canopy scale and at the leaf scale. Global Change Biology 1, 183–198.

McCree, K.J., 1970. An equation for the rate of dark respiration of white clover plants grown under controlled conditions. In: Setik, I. (Ed.), Prediction and Measurement of Photosynthetic Productivity. Centre for Agricultural Publishing and Documentation, pp. 221–229.

McMurtie, R.E., Leuning, R., Thomson, W.A., Wheeler, A.M., 1992. A model of canopy photosynthesis and water use incorporating a mechanisdtic formulation of leaf CO_2 exchange. For. Ecol. Manage.

McMurtie, R.E., Rook, D.A., Kelliher, F.M., 1990. Modelling the yield of Pinus radiata on a site limited by water and nitrogen. For. Ecol. Manage. 30, 381–413.

Molz, F.J., 1981a. Models of water transport in the soil–plant system: a review. Water Resour. Res. 17 (5), 1245–1260.

Molz, F.J., 1981b. Simulation of plant water uptake. In: Iskandar, I.K. (Ed.), Modeling Waste-Water Renovation by Land Application. John Wiley, New York.

Monteith, J.L., Unsworth, M.H., 1990. Principles of Environmental Physics. Edward Arnold, London.

Munns, R., Sharp, R.E., 1993. Involvement of abscisic acid in controlling plant growth in soils of low water potential. Aus. J. Plant Physiol 20, 425–437.

Murray, M.B., Cannel, M.G.R., Smith, R.I., 1989. Date of budburst of fifteen tree species in Britain following climatic warming. J. App. Ecol 26, 693–700.

Nadelhoffer, K.J., Raich, J.W., 1992. Fine root production estimates and belowground carbon allocation in forest ecosystems. Ecology 73, 1139–1147.

Nikolov, N.T. 1997. Mathematical Modeling of Seasonal Biogeophysical Interactions in Forest Ecosystems. PhD dissertation, Colorado State University, Fort Collins CO, 149 pp.

Nikolov, N.T., Massman, W.J., Shoettle, A.W., 1995. Coupling biochemical and biophysical processes at the leaf level: An equilibrium photosynthesis model for leaves of C_3 plants. Ecol. Modelling 80, 205–235.

Nikolov, N.T., Zeller, K.F., 1992. A solar radiation algorithm for ecosystem dynamic models. Ecol. Modelling 61, 149–168.

Oren, R., Schultze, E.D., Matyssek, R., Zimmermann, R., 1986. Estimating photosynthetic rate and annual carbon gain in conifers from specific leaf weight and leaf biomass. Oecologia 70, 187–193.

Perez, R., 1990. Modeling daylight availability and irradiance components from direct and global irradiance. Solar Energy 44 (5), 271–289.

Peterjohn, W.T., Mellilo, J.M., Steudler, P.A., Newkirk, K.M., Bowles, F.P., Aber, J.D., 1994. Responses of trace gas fluxes and N availability to experimentally elevated soil temperatures. Ecol. Applications 4 (3), 617–625.

Pielke, R.A., Avissar, R., 1990. Influence of landscape structure on local and regional climate. Landscape Ecol. 4, 133–155.

Potter, C.S., Wang, S., Nikolov, N.T., McGuire, A.D., Liu, J., King, A.W., Kimball, J.S., Grant, R.F., Frolking, S.E., Clein, J.S., Chen, J.M., Amthor, J.S., 2001. Comparison of boreal ecosystem model sensitivity to variability in climate and forest site parameters. J. Geophys. Res. 106 (33), 633–671,688.

Ross, J., 1981. The Radiation Regime and Architecture of Plant Stands. Dr. W. Junk Publishers, The Hague.

Running, S.W., Coughlan, J.C., 1988. A general model of forest eco-system processes for regional applications. I. Hydrologic balance, canopy gas exchange and primary production processes. Ecol. Modelling 42, 125–154.

Running, S.W., Gower, S.T., 1991. FOREST-BGC, A general model of forest ecosystem processes for regional applications. II. Dynamic carbon allocation and nitrogen budgets. Tree Physiol. 9, 147–160.

Ryan, M.G., 1991. Effects of climate change on plant respiration. Ecol. Applications 1 (2), 157–167.

Ryan, M.G., 1995. Foliar maintenance respiration of subalpine and boreal trees and shrubs in relation to nitrogen content. Plant, Cell and Environ. 18, 765–772.

Sampson, D.A., Smith, F.W., 1993. Influence of canopy architecture on light penetration in lodgepole pine (Pinus contorta var. latifolia) forests. Agric. For. Meteor. 64, 63–79.

Saxton, K.E., Rawls, W.J., Romberger, J.S., Papendick, R.I., 1986. Estimating generalized soil–water characteristics from texture. Soil Sci. Soc. Am. J. 50, 1031–1036.

Schlentner, R.E., Van Cleve, K., 1984. Relationships between CO_2 evolution from soil, substrate temperature, and substrate moisture in four mature forest types in interior Alaska. Can. J. For. Res. 15, 97–106.

Schoettle, A. W. 1989. Importance of Shoot Structure to Sunlight Interception and Photosynthetic Carbon Gain in *Pinus contorta* Crowns. PhD dissertation, University of Wyoming, pp.200.

Sellers, P.J., 1985. Canopy reflectance, photosynthesis and transpira-tion. Int. J. Remote Sensing 6 (8), 1335–1372.

Sellers, P.J., Mintz, Y., Sud, Y.C., Dalcher, A., 1986. A Simple Bio-sphere model (SiB) for use within General Circulation Models. J. Atmos. Sci. 46 (3), 505–531.

Sellers, P.J., Shuttleworth, W.J., Dorman, J.L., Dalcher, A., Roberts, J.M., 1988. Calibrating the Simple Biosphere Model for Amazonian tropical forest using field and remote sensing data. Part I: Average calibration with field data. J. App. Meteorol. 28 (8), 727–759.

Shaykewich, C.F., 1995. An appraisal of cereal crop phenology mod-elling. Can. J. Plant Sci. 75, 329–341.

Spitters, C.J.T., Toussaint, H.A.J.M., Goudriaan, J., 1986. Separating the diffuse and direct component of global radiation and its impli-cation for modeling canopy photosynthesis. Part I. Components of incoming radiation. Agric. For. Meteor. 38, 217–229.

Tardieu, F., 1993. Will increases in our understanding of soil–root

relations and root signalling substantially alter water flux models. Phil. Trans. R. Soc. Lond. 341, 57–66.

Tardieu, F., Davies, W.J., 1993a. Root-shoot communication and whole-plant regulation of water flux. In: Smith, J.A.C., Griffiths, H. (Eds.), Water Deficit. Plant Responses from Cell to Community. BIOS Sci. Publishers, Oxford, pp. 147–162.

Tardieu, F., Davies, W.J., 1993b. Integration of hydraulic and che-mical signalling in the control of stomatal conductance and water status of droughted plants. Plant, Cell and Environ. 16, 341–349.

Tardieu, F., Zhang, J., Gowing, D.J.G., 1993. Stomatal control by both [ABA] in the xylem sap and leaf water status: a test of a model for droughted or ABA-fed field-grown maize. Plant, Cell and Environ. 16, 413–420.

Turner, N.C., Waggoner, P.E., Rich, S.Removal of ozone from the atmosphere by soil and vegetationNature2501974486489

van Genuchten, M.Th., 1980. A closed form equation for predicting the hydraulic conductivity of unsaturated soils. Soil Sci. Soc. Am. J. 44, 892–898

van Pul, W.A.J., 1992. The flux of ozone to a maize crop and the underlying soil during a growing season. Ph.D. Thesis. Department of Meteorology, Agriculture University, Wageningen the Nether-lands.

Vereecken, H., Maes, J., Feyen, J., Darius, P., 1989. Estimating the soil moisture retention characteristic from texture, bulk density, and carbon content. Soil Sci. 148 (6), 389–403.

Vereecken, H., Maes, J., Feyen, J., 1990. Estimating unsaturated hydraulic conductivity from easily measured soil properties. Soil Sci. 149 (1), 1–12.

Wang, Y.P., Jarvis, G.P., 1988. Mean leaf angles for ellipsoidal incli-nation distribution. Agric. For. Meteor. 43, 319–321.

Wigmosta, M.S., Vail, L.W., Lettenmaier, D.P., 1994. A distributed hydrology-vegetation model for complex terrain. Water Resour. Res. 30 (6), 1665–1679.

Wu, Rong-Ling., 1994. Simulated optimal structure of a photo-synthetic system: implication for the breeding of forest crop ideo-type. Can. J. For. Re. 23, 1631–1638.

Zeller, K., Hehn, T., 1995. Ozone deposition in a snow-covered sub-alpine spruce-fir environment, In Biogeochemistry of Seasonally Snow-Covered Catchments, Proceedings of a Boulder Symposium, July 1995, IAHS Publ. no. 228, pp. 17–22.

Zeller, K., Niolov, N., 2000. Quantifying simultaneous fluxes of ozone, carbon dioxide and water vapor above a subalpine forest ecosystem. Environ. Pollution 107, 1–20.

Zhang, J., Davies, W.J., 1989. Sequential response of whole plant water relations to prolonged soil drying and the involvement of xylem sap ABA in the regulation of stomatal behavior of sunflower plants. New Physiologist 113, 167–174.